Published in final edited form as:
Biomaterials. 2013 August ; 34(26): 6229–6238. doi:10.1016/j.biomaterials.2013.04.061.

Post-Translational Regulation of a Hypoxia-Responsive VEGF Plasmid for the Treatment of Myocardial Ischemia

Young-Wook Won[1], **Arlo N. McGinn**[1,3], **Minhyung Lee**[2], **Kihoon Nam**[1], **David A. Bull**[4], and **Sung Wan Kim**[1,2,*]

[1]Center for Controlled Chemical Delivery (CCCD), Department of Pharmaceutics and Pharmaceutical Chemistry, University of Utah, Salt Lake City, UT, USA

[2]Department of Bioengineering, Hanyang University, Seoul, Republic of Korea

[3]Department of Pharmacology and Toxicology, University of Utah, Salt Lake City, UT, USA

[4]Division of Cardiothoracic Surgery, Department of Surgery, School of Medicine, University of Utah, Salt Lake City, UT, USA

Abstract

Vascular Endothelial Growth Factor (VEGF) gene therapy to promote therapeutic angiogenesis has been advanced as an alternative treatment for myocardial ischemia. The unregulated expression of VEGF and the use of viral vectors, however, have slowed the clinical development of angiogenic gene therapy. The development of clinically beneficial angiogenic gene therapy requires a disease-specific gene expression system and an efficient non-viral gene carrier. To address these requirements, we developed a new post-translationally regulated hypoxia-responsible VEGF plasmid, pβ-SP-ODD-VEGF, and a dendrimer type bio-reducible polymer, PAM-ABP. The efficacy of VEGF gene therapy with the PAM-ABP/pβ-SP-ODD-VEGF was evaluated and compared to the RTP-VEGF plasmid, a previously constructed hypoxia-inducible plasmid, in an ischemia/reperfusion (I/R) rat model. Cine magnetic resonance imaging was used to analyze the ischemia/reperfusion rats treated with either the PAM-ABP/pβ-SP-ODD-VEGF or the PAM-ABP/RTP-VEGF. The PAM-ABP/pβ-SP-ODD-VEGF treatment more effectively protected cardiomyocytes against apoptosis, preserved left ventricular (LV) function, and prevented LV remodeling compared to the PAM-ABP/RTP-VEGF-treated rats. These results suggest that the pβ-SP-ODD-VEGF with PAM-ABP may be efficacious in the treatment of acute ischemic heart disease.

Keywords

Myocardial infarct; Gene therapy; VEGF; PAM-ABP

*Corresponding author: S.W.Kim (sw.kim@pharm.utah.edu); 20 S 2030 E Rm 205 BPRB, Salt Lake City, UT 84112-5820, USA; Tel.: 1 801 581 6654; fax: 1 801 581 7848.

Introduction

Myocardial ischemia occurs when blood supply to the myocardium is reduced by stenosis or occlusion of a coronary artery [1]. Therapeutic angiogenesis induced by angiogenic growth factors, such as Vascular Endothelial Growth Factor (VEGF), may restore blood supply to the myocardium, preserving left ventricular (LV) function and preventing left ventricular remodeling [2]. Uncontrolled VEGF expression and secretion, however, may lead to severe side effects, including the development of vascular tumors that may cause heart failure [3]. VEGF over-expression in normoxic cardiomyocytes is also known to promote the progression of atherosclerosis. The severe side effects associated with the unregulated, constitutive expression of VEGF and the use of viral vectors has slowed the clinical development of VEGF gene therapy for the treatment of ischemic heart disease. We previously developed an ischemia-inducible VEGF-expressing plasmid, RTP-VEGF, that can promote angiogenesis and improve heart function following acute myocardial ischemia [2, 4]. A post-translationally regulated hypoxia-responsive plasmid, pβ-SP-ODD-VEGF, recently developed by our group, demonstrated higher levels of VEGF secretion compared with the RTP-VEGF under hypoxic conditions [5]. _ENREF_5 This is likely due to the signal peptide facilitating VEGF secretion, the presence of a stabilizing domain to protect the VEGF, and the presence of a furin-cleavage site to enhance the secretion of wild-type VEGF.

VEGF expression in response to hypoxia may be regulated at the transcription, the post-transcription, or the post-translation levels [6]. The RTP801 promoter used in the RTP-VEGF plasmid primarily regulates VEGF expression at the transcription level in ischemic tissues [7]. Unlike the RTP-VEGF, the pβ-SP-ODD-VEGF regulates VEGF secretion at the post-translation level by increasing the resident time of VEGF following expression and by facilitating the secretion of wild-type VEGF [6]. These different mechanisms of VEGF gene regulation resulted in the more efficient secretion of VEGF in the pβ-SP-ODD-VEGF-transfected cardiomyocytes. These findings suggest that differences in the level of the regulation of VEGF gene expression and secretion may lead to different outcomes in the treatment of myocardial ischemia.

Many types of non-viral vectors have been developed to address the safety issues encountered with the use of viral vectors. We have demonstrated the efficacy of an ischemia-inducible VEGF plasmid in an animal model of myocardial ischemia and the positive effects of Terplex and a Water-Soluble LipoPolymer(WSLP)/VEGF gene therapy on left ventricular function following myocardial infarction [4]. More recently, a non-viral gene carrier referred to as PAM-ABP, prepared by the conjugation of four arginine-grafted bio-reducible poly (disulfide amine) (ABP) molecules with poly (amido amine) (PAMAM) dendrimer, was developed by our group [8]. Since this polymer has only been studied *in vitro*, the *in vivo* efficacy of PAM-ABP with a therapeutic gene is unknown. In this study, we evaluated the efficacy of the PAM-ABP/pβ-SP-ODD-VEGF for the treatment of myocardial ischemia and compared it to the therapeutic efficacy of the RTP-VEGF plasmid in a rat model of myocardial ischemia.

Materials and Methods

All experiments were approved by the University of Utah's Institutional Animal Care and Use Committee and followed the guidelines provided by the National Institutes of Health in Guide for the Care and Use of Laboratory Animals.

Materials

Branched poly(ethylenimine) (bPEI, Mw: 25 kDa) and 3-[4,5-dimethylthiazol-2-yl]-2,5-diphenyltetrazolium bromide (MTT) were purchased from SigmaAldrich (St. Louis, MO). All cell culture products including fetal bovine serum (FBS), Dulbecco's phosphate buffered saline (DPBS), and Dulbecco's modified Eagle's medium (DMEM) were obtained from Invitrogen (GibcoBRL; Carlsbad, CA). Human VEGF ELISA kit was purchased from R&D Systems (Minneapolis, MN). Male Sprague Dawley rats (~300 g) were purchased from Charles River Laboratories International, Inc. (Wilmington, MA, USA).

Plasmid Preparation

The pβ-SP-ODD-VEGF and RTP-VEGF plasmids used in this study were prepared as described previously [5, 7]. Briefly, the VEGF cDNA, the ODD cDNA, and the SP cDNA were amplified by PCR using pSV-VEGF, pSV-Luc-ODD, and pUAS-SP-GLP-1 as templates, respectively. The furin recognition site was inserted upstream of the start codon of the VEGF cDNA. The amplified VEGF cDNA was inserted into the pβ, and the ODD cDNA was inserted upstream of the furin-VEGF cDNA. Finally, the SP cDNA was inserted into pβ-ODD-VEGF, producing pβ-SP-ODD-VEGF. The RTP801-VEGF plasmid, a hypoxia-inducible VEGF plasmid developed previously by our group, was used as a positive control for comparison of the efficacy of a hypoxia-inducible VEGF plasmid in a rat myocardial model.

PAM-ABP Synthesis

PAM-ABP was synthesized as previously detailed [8]. In brief, ABP was first synthesized as described previously [9]. The mixture of SPDP and ABP was reacted for 1 hour, and then dialyzed using a dialysis membrane (MWCO = 1 kDa, Spectrum Laboratories, Inc., Rancho Dominguez, CA). PAMAM dissolved in phosphate buffered saline was reacted with Traut's reagent to introduce sulfhydryl groups for 2 h. The PAMAM-SH was purified and lyophilized. The ABP-SPDP was mixed with the PAMAM-SH, and the reaction was terminated by dialysis when no release of pyridine-2-thione was observed under UV.

In Vitro Transfection

H9C2 cells were cultured in DMEM containing 10% FBS and 1% antibiotics at 37°C under 5% CO_2. The cells were seeded on 24-well plates at a density of 2.0×10^4 cells/well. After 24 hours of incubation, the culture media was replaced with plain media containing PAMAB/pDNA or PEI/pDNA polyplexes prepared by mixing 1 μg pDNA and 5, 10, 15 μg PAM-ABP or 1 μg PEI. After 4 hours, the cells were washed with PBS and cultured with DMEM. For the creation of hypoxic conditions, the culture plates were placed in a hypoxia chamber filled with 5% CO_2, 94% N_2, and 1% O_2. The cell culture media was collected 48 hours after transfection and the cells were treated with MTT for the cell viability assay. The amount of VEGF production and secretion were quantified using a VEGF ELISA kit (R&D Systems; Minneapolis, MN) according to the manufacturer's protocol.

Rat Ischemia/Reperfusion Model

All animal experiments were performed according to protocols approved by the University of Utah's Institutional Animal Care and Use Committee. Male Sprague Dawley rats were anesthetized in an induction chamber delivering 4% isoflurane, sedated with an intramuscular injection of 40 mg/kg ketamine, and had their left chests shaved. The rats were re-anesthetized under 4% isoflurane ten minutes after the ketamine injection and quickly intubated by hanging their incisors and inserting a catheter over a guide wire past the vocal cords into the trachea. The rats were transferred to an operating table equipped with a warm water pad and anesthesia was maintained with a rodent ventilator delivering

2% isoflurane at a tidal volume of 1.5–2.0 mL and a respiration rate of 60–70 breaths per minute. A small incision was made in the 5th intercostal space and the ribs were spread using a retractor to expose the chest cavity. The left lung was gently collapsed and retracted to visualize the heart using a wet 2" × 2" gauze pad. After widely incising the pericardium, the left anterior descending artery (LAD) was ligated 2 mm from the anterior tip of the left atrial appendage by passing a 6–0 prolene suture under the LAD. The suture was threaded through a 2 cm length of PE-50 tubing (Becton Dickinson, Franklin Lakes, NJ) and then removed 30 minutes after the ligation. Blanching of the myocardium and visible dyskinesia of the anterior wall of the left ventricle were observed to confirm successful ligation of the LAD. The rats were randomly assigned to one of three experimental groups: 1) ligation only (n=6); 2) injection of PAM-ABP/pβ-SP-ODD-VEGF (n=6); and 3) injection of PAM-ABP/RTP-VEGF (n=6). After assignment, the suture was removed from the myocardium and 100 μl PBS containing 25 μg of plasmid DNA complexed with 125 μg PAB-ABP (1:5 w/w) was injected in 4 sites of the myocardium (3 sites around the ischemic border zone and 1 site in the central infarct zone). The chest was closed in layers and the animal was allowed to recover under a warming lamp and given injections of pain alleviating medication (Buprenorphine) and antibiotics (Cefazolin). The sham surgery control animals received a full thoracotomy with exposure of the heart and had a suture passed under the LAD, but no ligation of the LAD. A licensed veterinarian carefully observed the rats for signs of pain on a regular basis after surgery.

Magnetic Resonance Imaging (MRI)

Cardiac Cine-MRI was performed to determine changes in indices of heart function in all animals two weeks after surgery. The rats were placed prone on a pressure sensor to monitor respiration and a pulse oximeter was attached to the rat's foot. A Bruker Biospec 7T/30 cm MRI operated with Bruker AVANCE II electronics (Bruker BioSpin MRI GmbH, Ettlingen, Germany) with a Bruker birdcage quadrature resonator (72 mm internal diameter) was used to monitor the heart for signal transmission and reception. The images were acquired using retrospectively gated fast-low-shot-angle (FLASH) pulse sequences in CINE mode. The instrument settings were as follows: repetition time (TR) = 72 ms, echo time (TE) = 3 ms, flip-angle 10°, number of repetitions = 100, field of view (FOV) = 40 mm × 55 mm, matrix size = 196 × 96 zero-padded to 392 × 192 yielding an effective in-plane resolution of 102 × 286 microns. A total of 7 short-axis scans (slice thickness = 1.5 mm, number of movie frames = 10) were acquired. Images were reconstructed using Bruker's Intragate software and exported as DICOM files for analysis. The CINE MRI sequences were used to analyze left ventricular ejection fraction, wall thickness, and volume using Segment software v1.8 (Segment; http://segment.heiberg.se) [10]. An investigator blinded to the treatment groups analyzed the left ventricle in a semi-automated manner. Wall thickness was measured at the mid-ventricular level in a short-axis view at end diastole and end systole.

Histology and Immunohistochemistry

The day of MRI analysis, the rats were sacrificed by inhalation of an overdose of isoflurane. The hearts were excised, washed, and perfused with 20 mL of Heparin-PBS, 20 mL of 2.56M KCl, and 20 mL of 10% formalin. The hearts were fixed in 10% formalin at 25 °C for 72 hours, and then transferred to 70% EtOH until sectioning. The hearts were sectioned along the short axis into 2 mm slices using an acrylic tissue matrix (Zivic Instruments; Pittsburg, PA) and embedded in paraffin. The paraffin-embedded heart section slices were air-dried at room temperature and placed in a 60 °C oven for 30 min to melt the paraffin. De-paraffinization was performed by three washes of xylene (5 minutes each), rehydration in ethanol (100% × 2, 95% × 2, 70% × 1, 1 minute each), and washing with dH2O. All histologic and immunohistochemical staining was performed at 37 °C using an automated immunostainer (BenchMark® XT, Ventana Medical Systems, Tucson, AZ).

Masson's trichrome staining was used to determine the size of the myocardial infarction. The total epicardial area of the left ventricle, the total endocardial area of the left ventricle, and the total collagen-stained area were determined by ImageJ (NIH, Bethesda, MA). The percent infarct was calculated using the following equation: Infarct size (%)=collagen-stained area/(epicardial area – endocardial area)×100.

To evaluate the arteriolar and capillary density, the heart slices were immunohistochemically stained using α-SMA and endocardial cell specific CD31 (Purified Mouse Anti-Rat CD31, Abcam). Additional heart slices were stained using a rabbit anti-rat CRIP2 antibody (LSBio; Seattle, WA) and anti-human VEGF antibody. Slices were incubated at room temperature with the primary antibodies for 20 minutes followed by the secondary antibody for 20 minutes. The sections were analyzed using the IView DAB (3-3' diaminobenzidine) detection kit-research (Ventana Medical Systems; Tucson, AZ), a Streptavidin-HRP system, utilizing DAB as the chromogen. The sections were counterstained with hematoxylin (Ventana Medical Systems; Tucson, AZ) for 4 min. The CD31-positive capillaries and α-SMA-positive arterioles in the border zone of infarct were counted in five random high power fields in each heart using Aperio ImageScope V11.2.0.780 (Aperio Technologies, Inc., Vista, CA) and calculated as the average number of capillaries or arterioles per mm^2. The number of CRIP2- and VEGF-positive cells were also counted and calculated as described above.

The determination of apoptosis was performed using a commercially available ApopTag® Fluorescein Apoptosis Detection Kit (Millipore, Billerica, MA) according to the manufacturer's instructions. Apoptosis in the border zone was imaged at 40 × magnification using an Olympus FV1000 confocal fluorescent microscope (Olympus, Center Valley, PA) and quantified by counting positively stained cells from five random high power fields for each animal.

The entire immunohistochemistry and H&E slides were scanned using an Aperio CS Scanscope (Aperio Technologies, Inc., Vista, CA) at 20× magnification. For the histological analysis, high power fields were randomly chosen in the infarct border zone by an investigator blinded to the treatment groups. The analysis of all images was carried out with NIH ImageJ (NIH, Bethesda, MD).

Results

VEGF Plasmid Transfection using PAM-ABP

The transfection efficiency of the VEGF plasmid using PAM-ABP was evaluated at a variety of PAM-ABP:DNA weight ratios to determine the most efficient and non-toxic weight ratio. The relative secretion of VEGF for all weight ratios of PAM-ABP was ~3 fold higher compared to bPEI (Fig. 1a). The relative secretion of VEGF with PAM-ABP was ~2.8-fold at a weight ratio of 5, ~3-fold higher at a weight ratio of 10, and ~2.8-fold higher at a weight ratio of 15. Evaluating the cellular toxicity of any polymer is crucial prior to *in vivo* study. Cellular viability under the same test conditions used for VEGF plasmid transfection was determined by MTT assay. The relative cellular viabilities in the PAM-ABP/pβ-SP-ODD-VEGF-treated groups were ~95% at a weight ratio of 5 and ~90% at weight ratios of 10 and 15, while cellular viability in the bPEI group was only ~50% (Fig. 1b). We decided to use the PAM-ABP at a weight ratio of 5 for VEGF plasmid transfection because there was no significant difference in VEGF secretion between the tested weight ratios and the cellular toxicity of the PAM-ABP was minimal at this weight ratio.

Infarct Size and Cardiomyocyte Apoptosis

Ligation of the left anterior descending coronary artery causes acute myocardial ischemia and can progress to infarction which, in turn, results in the death of cardiomyocytes, collagen deposition and myocardial fibrosis. The presence of collagen deposition correlating to areas of infarction can be detected by Masson's trichrome (MT) staining (Fig. 2a). There was no evidence of collagen deposition in the thoracotomy only group. There was only a small area of collagen deposition in the pβ-SP-ODD-VEGF group, while there were large areas of fibrosis and scarring in the ischemia/reperfusion (I/R) control group and the RTP-VEGF treatment group. Calculating the ratio of the area occupied by fibrotic tissue to the total cross-sectional area of the left ventricle, the area of infarction was ~28% in the I/R control group, ~19% in the RTP-VEGF group, and only ~7% in the pβ-SP-ODD-VEGF group (Fig. 2b). Therefore, the areas of infarction were significantly smaller in the pβ-SP-ODD-VEGF-treated hearts compared to the I/R control group and the RTP-VEGF treated hearts.

TUNEL-positive cells indicate the presence of apoptotic cardiomyocytes in the border zone of the infarct (Fig. 2a). The average number of TUNEL-positive cardiomyocytes in five random regions was ~13 in the thoracotomy only group, ~110 in the I/R control group, ~40 in the pβ-SP-ODD-VEGF treatment group, and ~125 in the RTP-VEGF treatment group (Fig. 2c). The PAM-ABP/pβ-SP-ODD-VEGF-treated hearts demonstrated a significant reduction in infarct size and apoptotic cardiomyocytes compared to the RTP-VEGF treatment group.

Cardiomyocyte Hypertrophy and Density

Analysis of the cardiomyocyte surface area and density in the cross-sectioned heart slices provides information concerning the degree of remodeling at the cellular level (Fig. 2a). The cross-sectional area of cardiomyocytes in the I/R control group (~650 μm^2) was larger than the cross-sectional area of cardiomyocytes in the thoracotomy only group (~250 μm^2), the pβ-SP-ODD-VEGF treatment group (~320 μm^2), and the RTP-VEGF treatment group (~450 μm^2) (Fig. 2d). The cardiomyocytes in the PAM-ABP/pβ-SP-ODD-VEGF treatment group were significantly smaller than the cardiomyocytes in the I/R control group and slightly larger than the cardiomyocytes in the thoracotomy only group. The cardiomyocytes in the PAM-ABP/pβ-SP-ODD-VEGF treatment group were significantly smaller than the cardiomyocytes in the PAM-ABP/RTP-VEGF treatment group. Similar results were observed in the analysis of cardiomyocyte density. The density of cardiomyocytes was decreased significantly in the I/R control group (~1100 mm^2) compared to all the other study groups, i.e. ~2300 mm^2 in the thoracotomy only group, ~2000 mm^2 in the pβ-SP-ODD-VEGF treatment group, and ~1400 mm^2 in the RTP-VEGF treatment group (Fig. 2e).

MRI Analysis

Two weeks after surgery, left ventricular function was assessed by cineMRI. The yellow arrows in Fig. 3 indicate the area of infarction following ligation of the coronary artery. When compared with the thoracotomy control group, the cross-sectional heart images of the anterior wall of the left ventricle showed a decrease in left ventricular function wall in all the study groups subjected to ischemia/reperfusion injury (Fig. 3a–d). Thinning of the anterior wall of the left ventricle was most significant in the ischemia/reperfusion control group. In comparison, the PAM-ABP/pβ-SP-ODD-VEGF-treated hearts maintained near-normal thickness of the anterior wall while the RTP-VEGF-treated hearts demonstrated partial preservation of the anterior wall. The change in LV wall thickness was also observed throughout one cardiac cycle at the mid-ventricular level. To analyze left ventricular wall motion, the left ventricle was divided into four sectors. Among the four sectors of the left ventricle, sector 3 reproducibly contained the area of infarction in our rat models. In sector

3, the thickness of the left ventricular wall of the PAM-ABP/pβ-SP-ODD-VEGF-treated rats (Fig. 4c) approximated the wall seen in the thoracotomy only rats (Fig. 4a), and was significantly greater than the left ventricular wall thickness in the ischemia/reperfusion rats (Fig. 4b) and the PAM-ABP/RTP-VEGF treated rats throughout the cardiac cycle (Fig. 4d). LV wall thicknesses in sector 3 at end diastole and end systole were compared in all groups (Fig. 4e). A dramatic change in LV wall thickness between end diastole and end systole was observed in the thoracotomy only and the pβ-SP-ODD-VEGF-treated rats, while there was only a slight difference in the LV wall thickness in the I/R control and the RTP-VEGF treatment groups. These results demonstrate that treatment with the PAM-ABP/pβ-SP-ODD-VEGF preserved the muscular structure and prevented remodeling of the left ventricle following ischemia/reperfusion injury.

Functional Analysis

In concordance with the LV wall thickness results, a dramatic decrease in left ventricular function was observed in the ischemia/reperfusion control group and the RTP-VEGF treatment group compared to the thoracotomy only group (Fig. 5a). The left ventricular ejection fraction in the thoracotomy only group was ~80%. Treatment with PAM-ABP/pβ-SP-ODD-VEGF maintained the left ventricular ejection fraction at ~75%, while the ejection fraction in the RTP-VEGF treatment group declined to ~60%. The ejection fraction in the ischemia/reperfusion control group was ~58%. Therefore, the ejection fraction in the pβ-SP-ODD-VEGF group was near-normal and significantly improved compared to the I/R control group, while the ejection fraction was only negligibly improved in the RTP-VEGF treatment group compared to the I/R control group. Stroke volume analysis of the pumping efficiency of the heart demonstrated a similar pattern to the ejection fraction measurements (Fig. 5b). We analyzed the left ventricular volume at end diastole and at end systole. There was no significant difference in the end diastolic volume (EDV) when comparing all the groups (Fig. 5c). Unlike the EDV determination, the end systolic volume (ESV) differed significantly between the ischemia/reperfusion control group and the thoracotomy only group (Fig. 5d). The ESV was only slightly increased in the PAM-ABP/pβ-SP-ODD-VEGF treatment group (~55 μl) compared to the thoracotomy only group (~50 μl), and was significantly less than the ESV in the PAM-ABP/RTP-VEGF treatment group (~95 μl) and the ischemia/reperfusion control group (~100 μl). Additionally, the cardiac output data was concordant with the ejection fraction data and the stroke volume data (Fig. 5e). These results demonstrate that the PAM-ABP/pβ-SP-ODD-VEGF treatment prevented the LV remodeling seen in both the ischemia/reperfusion control group and the RTP-VEGF treatment group.

Vascular Density

The presence of arterioles in the border zone of the infarct was detected by immunohistochemical staining with an anti-smooth muscle α-actin (SMA) antibody (Fig. 6a). The SMA-positive arterioles present in five random areas in the border zone of infarct were counted and the vascular density calculated as the average number of arterioles per mm^2 high power field (Fig. 6c). This immunostaining revealed that there were more arterioles present in the PAM-ABP/pβ-SP-ODD-VEGF-treated myocardium (~13 arterioles/mm^2) than in any of the other groups. The number of arterioles was also increased in the ischemic myocardium treated with the RTP-VEGF (~7 arterioles/mm^2) compared to the thoracotomy only and the I/R control groups.

Capillary endothelial cells were detected using an anti-CD31 antibody (Fig. 6b). CD31-positive capillaries were counted and calculated in the same manner as the SMA analysis (Fig. 6d). The mean number of capillaries positive for CD31 were ~3 in the thoracotomy only group and the I/R control group, ~8 in the RTP-VEGF treatment group, and ~20 in the pβ-SP-ODD-VEGF treatment group. As the increase in the number of arterioles and

capillaries present would be expected to be in direct proportion to the amount of VEGF released, we conclude that the pβ-SP-ODD-VEGF secreted more VEGF into the ischemic myocardium than the RTP-VEGF.

VEGF Expression

To evaluate VEGF expression in the border zone of the infarct, immunohistochemical staining with anti-human VEGF antibody was performed (Fig. 7a). Cardiomyocytes positive for hVEGF were detected even in the thoracotomy only group and the ischemia/reperfusion group. This is due to the cross-reactivity of the hVEGF antibody with rat VEGF. The VEGF-positive cardiomyocytes were counted and the average number of positive cells was calculated in the same manner as the SMA analysis described above. The PAM-ABP/pβ-SP-ODD-VEGF-treated ischemic myocardium demonstrated more VEGF-positive cells than any of the other groups (Fig. 7b). The number of VEGF-positive cells was also increased in the RTP-VEGF treatment group but to a significantly lesser degree than the pβ-SP-ODD-VEGF treatment group. The percentage of VEGF positive cells per mm^2 of cardiomyocyte area was ~13% in the thoracotomy only group, ~14% in the ischemia/reperfusion control group, ~23% in the RTP-VEGF treatment group, and ~30% in the pβ-SP-ODD-VEGF treatment group. These findings demonstrate that the pβ-SP-ODD-VEGF delivered using the bio-reducible polymer, PAM-ABP, was more effective at transfecting cardiomyocytes and promoting the secretion of VEGF than the RTP-VEGF delivered using the same PAM-ABP polymer.

CRIP2 Expression

The stimulation of smooth muscle development following ischemia/reperfusion injury was evaluated in the cross-sectioned heart by using an anti-CRIP2 antibody to detect the presence of CRIP2, one of the cysteine-rich LIM-only proteins expressed during cardiovascular development (Fig. 8a) [11]. Determination of the percentage of the cardiomyocyte area that was positive for CRIP2 was calculated in the same manner as the method for SMA described above. The ischemic myocardium treated with the PAM-ABP/pβ-SP-ODD-VEGF demonstrated a significant increase in the number of cardiomyocytes positive for CRIP2 (Fig. 8b). There was also an increase in the number of CRIP2-positive cells in the RTP-VEGF treatment group and in the ischemia/reperfusion control group. The percentage of CRIP2-positive cells per mm^2 of cardiomyocyte area was ~7% in the thoracotomy only group, ~11% in the ischemia/reperfusion control group, ~15% in the RTP-VEGF treatment group and ~37% in the pβ-SP-ODD-VEGF treatment group. These results are consistent with the VEGF expression analysis data and indicate that VEGF transfection using PAM-ABP can also stimulate the development of smooth muscle in ischemic myocardium.

Discussion

Many studies have reported that VEGF gene therapy can improve heart function and prevent left ventricular remodeling following acute ischemia/reperfusion injury [12]. VEGF is a key molecule in the pathway of neovascularization and is secreted from ischemic cardiomyocytes [13]. In this setting, VEGF may act in either an autocrine and paracrine manner to limit myocardial dysfunction and left ventricular remodeling [14]. The two primary requirements for VEGF gene therapy for the treatment of myocardial ischemia are: 1) an effective delivery vehicle; and 2) a VEGF-expressing plasmid.

Cationic polymers have the potential to be ideal carri_ENREF_8ers for gene delivery. We recently developed a bio-reducible dendrimer-type polymer, PAM-ABP, which has high transfection efficiency and low toxicity compared to both bPEI and other reducible polymers

[8]. The high charge density of PAM-ABP leads to a higher transfection efficiency than PEI at all weight ratios and negligible toxicity. We chose to use PAM-ABP at a weight ratio of 5 for our *in vivo* studies as this weight ratio provided for the optimal balance of high transfection efficiency and minimal toxicity.

The process of remodeling of the left ventricle begins immediately after an acute ischemic insult. The extent of remodeling correlates with the size of the infarct and the decline in cardiac function [15]. Oxidative stress resulting from rapid metabolic changes in the early stages of ischemia plays a crucial role in cardiomyocyte apoptosis and fibrosis of myocardium [16]. The extent of cardiomyocyte loss in the early stages following an acute MI correlates directly with the subsequent degree of left ventricular remodeling and the decline in cardiac function. This suggests that preventing the loss of cardiomyocytes in the early stages of an acute MI is necessary to achieve long-term efficacy in the treatment of ischemic heart disease. The protective effects of VEGF gene therapy in the setting of acute myocardial ischemia are due not only to the induction of angiogenesis but also to the prevention of apoptosis of cardiomyocytes. The extent of the inhibition of apoptosis is directly correlated with the amount of VEGF released [17, 18]. The significant reduction in the number of apoptotic cardiomyocytes and the size of the myocardial infarcts in the PAM-ABP/pβ-SP-ODD-VEGF treated hearts demonstrate that the pβ-SP-ODD-VEGF is more efficacious at preventing left ventricular remodeling and preserving left ventricular function than the RTP-VEGF. This is consistent with our previously published VEGF secretion data [5] showing more efficient secretion of wild-type VEGF using the pβ-SP-ODD-VEGF plasmid compared to the RTP-VEGF plasmid. This high level of VEGF expression in the PAM-ABP/pβ-SP-ODD-VEGF treatment group, as confirmed by immunohistochemical analysis (Fig. 7), facilitates the formation of capillaries and arterioles (Fig. 6). In addition, a direct correlation between VEGF secretion and the development of smooth muscle was observed (Fig. 8), suggesting that the PAM-ABP/pβ-SP-ODD-VEGF not only inhibits cardiomyocyte apoptosis, but also induces the development of smooth muscle in ischemic myocardium.

The wall thickening measurements, the morphological analysis, and the immunohistochemical analysis exhibit insights into the reasons for the decline in left ventricular function. A significant loss of cardiomyocytes and a significant decline in left ventricular function were observed in the ischemia/reperfusion control group and the RTP-VEGF treatment group. Analysis of the left ventricular wall function over the course of the cardiac contractility cycle demonstrated that the segmental wall motion of the infarct region was less than that of the unaffected normal regions. This decline in wall motion is due to cardiomyocyte apoptosis and the replacement of cardiomyocytes with non-contractile fibrotic tissue. The PAM-ABP/pβ-SP-ODD-VEGF-treated rats demonstrated preservation of near-normal wall motion in the region of the infarct.

The difference in efficacy between the RTP-VEGF and the pβ-SP-ODD-VEGF is, at least in part, due to where the hypoxia-responsive regulation of gene expression occurs. The RTP801 promoter includes hypoxia-inducible factor-1 (HIF-1) binding sites and stimulating protein-1 (Sp1) that is up regulated under hypoxic conditions. Formation of a multi-protein complex of Sp1 with HIF-1 and Smad3, used as a co-activator and adaptor protein, results in a Sp1-Smad3-HIF-1 complex on the RTP801 promoter that works to enhance gene expression under hypoxic conditions [6, 19]. Unlike the RTP801, the pβ-SP-ODD-VEGF composed of the signal peptide, the ODD domain, and the furin cleavage site regulates VEGF secretion in response to hypoxic conditions at the post-translational level [5]. The ODD domain stabilizes VEGF in hypoxic cells, while the furin site is cleaved by furin enzyme in the Golgi apparatus, leading to the production of wild-type VEGF. The SP domain then facilitates the exogenous secretion of this wild-type VEGF, which is the most

potent form of VEGF [6, 20, 21]. This hypoxia-responsive regulation of VEGF expression and secretion is the mechanism underlying the differences in the therapeutic effects of the pβ-SP-ODD-VEGF and the RTP-VEGF observed in this study.

Conclusions

We have demonstrated that hypoxia-responsive VEGF gene therapy improves left ventricular function and prevents left ventricular remodeling following acute myocardial ischemia by inhibiting apoptosis of cardiomyocytes and promoting angiogenesis. When comparing two different hypoxia-responsive regulation systems, i.e. transcriptional versus post-translational regulation, pβ-SP-ODD-VEGF, the post-translationally regulated hypoxia-responsive plasmid, was more efficacious than RTP-VEGF, a transcriptionally regulated hypoxia-inducible system, at ameliorating the effects of ischemia/reperfusion injury in a rat model. The PAM-ABP/pβ-SP-ODD-VEGF shows promise as a potential novel therapy for the treatment of myocardial ischemia and infarction.

Acknowledgments

This work was supported by NIH grant HL065477 (SW Kim). The work of Minhyung Lee was supported by the Ministry of Education, Science and Technology, Korea (2012K001394).

References

[1]. McGinn AN, Nam HY, Ou M, Hu N, Straub CM, Yockman JW, et al. Bioreducible polymer-transfected skeletal myoblasts for VEGF delivery to acutely ischemic myocardium. Biomaterials. 2011; 32:942–9. [PubMed: 20970850]

[2]. Yockman JW, Choi D, Whitten MG, Chang CW, Kastenmeier A, Erickson H, et al. Polymeric gene delivery of ischemia-inducible VEGF significantly attenuates infarct size and apoptosis following myocardial infarct. Gene Ther. 2009; 16:127–35. [PubMed: 18784748]

[3]. Schwarz ER, Speakman MT, Patterson M, Hale SS, Isner JM, Kedes LH, et al. Evaluation of the effects of intramyocardial injection of DNA expressing vascular endothelial growth factor (VEGF) in a myocardial infarction model in the rat--angiogenesis and angioma formation. J Am Coll Cardiol. 2000; 35:1323–30. [PubMed: 10758976]

[4]. Bull DA, Bailey SH, Rentz JJ, Zebrack JS, Lee M, Litwin SE, et al. Effect of Terplex/VEGF-165 gene therapy on left ventricular function and structure following myocardial infarction. VEGF gene therapy for myocardial infarction. J Control Release. 2003; 93:175–81. [PubMed: 14636723]

[5]. Won YW, Lee M, Kim HA, Bull DA, Kim SW. Post-translational regulated and hypoxia-responsible VEGF plasmid for efficient secretion. J Control Release. 2012; 160:525–31. [PubMed: 22450332]

[6]. Kim HA, Mahato RI, Lee M. Hypoxia-specific gene expression for ischemic disease gene therapy. Adv Drug Deliv Rev. 2009; 61:614–22. [PubMed: 19394379]

[7]. Lee M, Bikram M, Oh S, Bull DA, Kim SW. Sp1-dependent regulation of the RTP801 promoter and its application to hypoxia-inducible VEGF plasmid for ischemic disease. Pharm Res. 2004; 21:736–41. [PubMed: 15180327]

[8]. Nam HY, Nam K, Lee M, Kim SW, Bull DA. Dendrimer type bio-reducible polymer for efficient gene delivery. J Control Release. 2012; 160:592–600. [PubMed: 22546681]

[9]. Choi D, Hwang KC, Lee KY, Kim YH. Ischemic heart diseases: current treatments and future. J Control Release. 2009; 140:194–202. [PubMed: 19563848]

[10]. Heiberg E, Wigstrom L, Carlsson M, Bolger AF, Karlsson M. Time resolved three-dimensional automated segmentation of the left ventricle. Computers in Cardiology. 2005; 2005:599–602.

[11]. Chang DF, Belaguli NS, Iyer D, Roberts WB, Wu SP, Dong XR, et al. Cysteine-rich LIM-only proteins CRP1 and CRP2 are potent smooth muscle differentiation cofactors. Dev Cell. 2003; 4:107–18. [PubMed: 12530967]

[12]. Sutton MG, Sharpe N. Left ventricular remodeling after myocardial infarction: pathophysiology and therapy. Circulation. 2000; 101:2981–8. [PubMed: 10869273]

[13]. Haynesworth SE, Baber MA, Caplan AI. Cytokine expression by human marrow-derived mesenchymal progenitor cells in vitro: effects of dexamethasone and IL-1 alpha. J Cell Physiol. 1996; 166:585–92. [PubMed: 8600162]

[14]. Giordano FJ, Gerber HP, Williams SP, VanBruggen N, Bunting S, Ruiz-Lozano P, et al. A cardiac myocyte vascular endothelial growth factor paracrine pathway is required to maintain cardiac function. Proc Natl Acad Sci U S A. 2001; 98:5780–5. [PubMed: 11331753]

[15]. Struthers AD. Pathophysiology of heart failure following myocardial infarction. Heart. 2005; 91(Suppl 2):ii14–6. discussion ii31, ii43–8. [PubMed: 15831601]

[16]. Won YW, Kim JK, Cha MJ, Hwang KC, Choi D, Kim YH. Prolongation and enhancement of the anti-apoptotic effects of PTD-Hsp27 fusion proteins using an injectable thermo-reversible gel in a rat myocardial infarction model. J Control Release. 2010; 144:181–9. [PubMed: 20153787]

[17]. Dai Y, Xu M, Wang Y, Pasha Z, Li T, Ashraf M. HIF-1alpha induced-VEGF overexpression in bone marrow stem cells protects cardiomyocytes against ischemia. J Mol Cell Cardiol. 2007; 42:1036–44. [PubMed: 17498737]

[18]. Gupta K, Kshirsagar S, Li W, Gui L, Ramakrishnan S, Gupta P, et al. VEGF prevents apoptosis of human microvascular endothelial cells via opposing effects on MAPK/ERK and SAPK/JNK signaling. Exp Cell Res. 1999; 247:495–504. [PubMed: 10066377]

[19]. Xu Q, Ji YS, Schmedtje JF Jr. Sp1 increases expression of cyclooxygenase-2 in hypoxic vascular endothelium. Implications for the mechanisms of aortic aneurysm and heart failure. J Biol Chem. 2000; 275:24583–9. [PubMed: 10825178]

[20]. Koditz J, Nesper J, Wottawa M, Stiehl DP, Camenisch G, Franke C, et al. Oxygen-dependent ATF-4 stability is mediated by the PHD3 oxygen sensor. Blood. 2007; 110:3610–7. [PubMed: 17684156]

[21]. Kim HA, Kim K, Kim SW, Lee M. Transcriptional and post-translational regulatory system for hypoxia specific gene expression using the erythropoietin enhancer and the oxygen-dependent degradation domain. J Control Release. 2007; 121:218–24. [PubMed: 17628167]

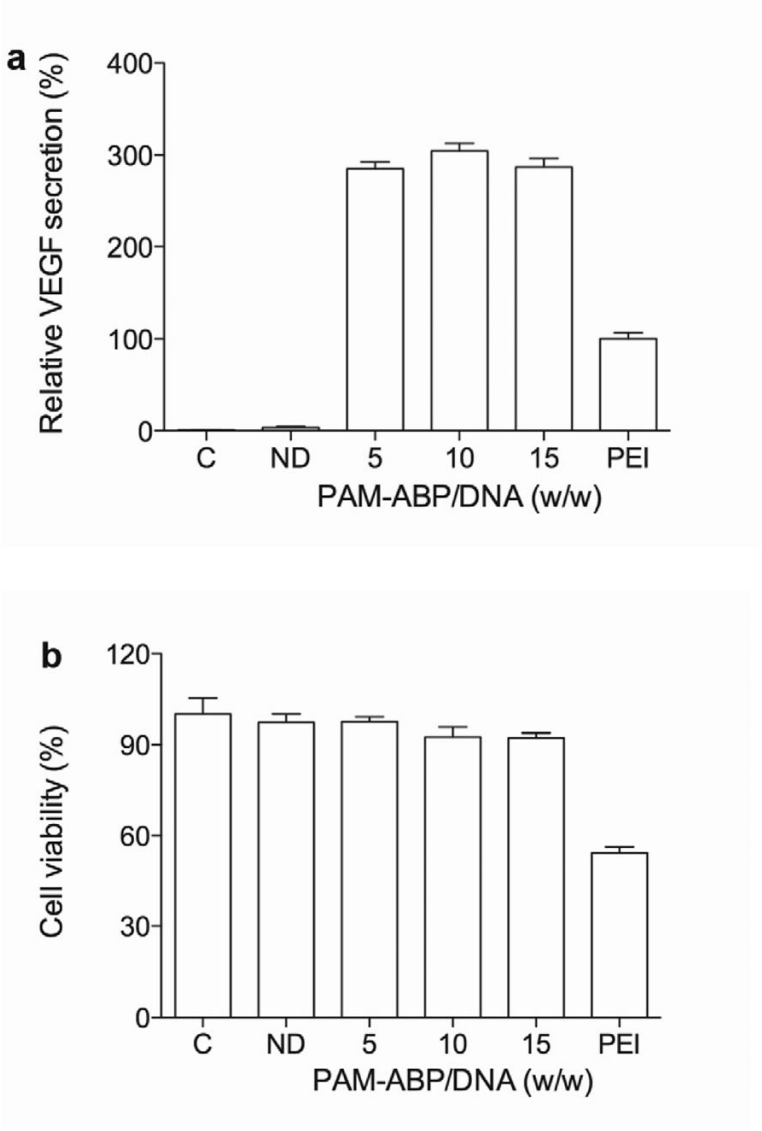

Figure 1.

Optimization of pVEGF transfection using PAM-ABP. (a) The pβ-SP-ODD-VEGF was transfected to H9C2 cells using PAM-ABP at three different weight ratios and branched PEI (25 kDa), a positive control, at a weight ratio of 1. VEGF secretion was quantitatively determined using an ELISA kit at 48 hours post-transfection. (b) Cell viability was measured by MTT assay under the same conditions used in (a). The data are presented as the mean ± the SD of three independent measurements. C and ND indicate control and naked plasmid DNA, respectively.

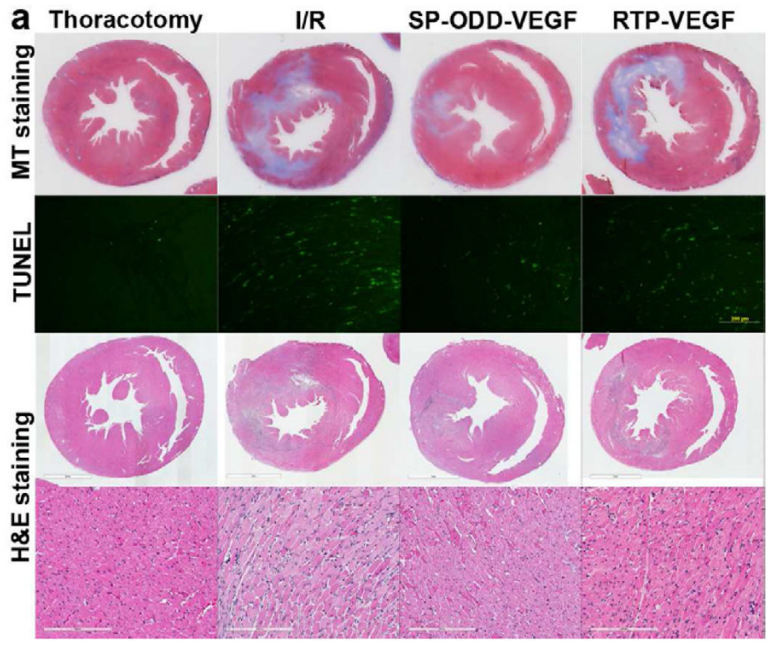

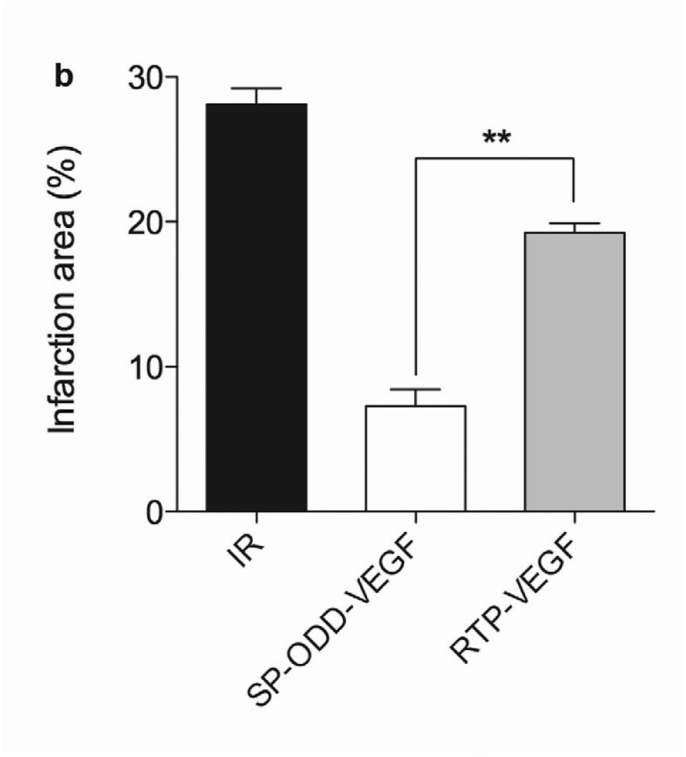

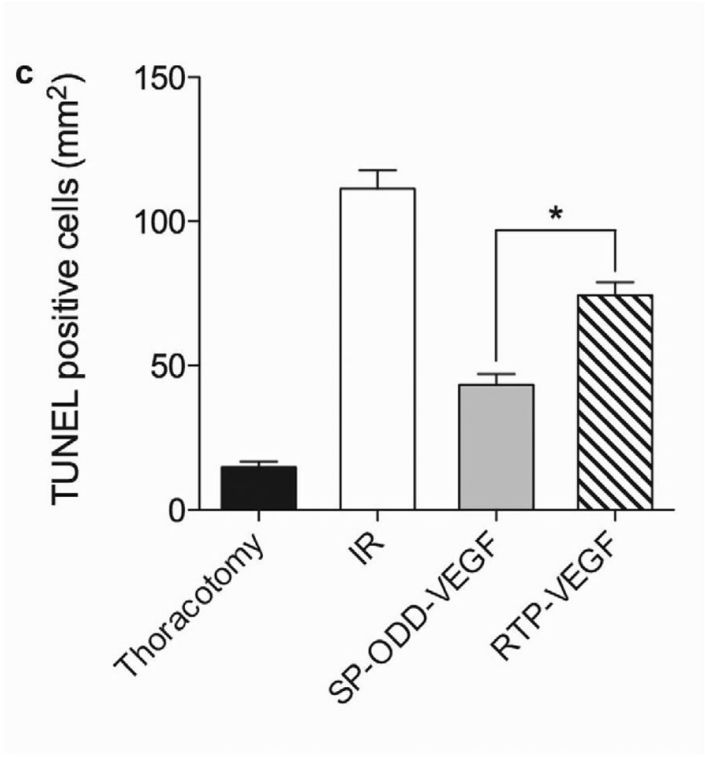

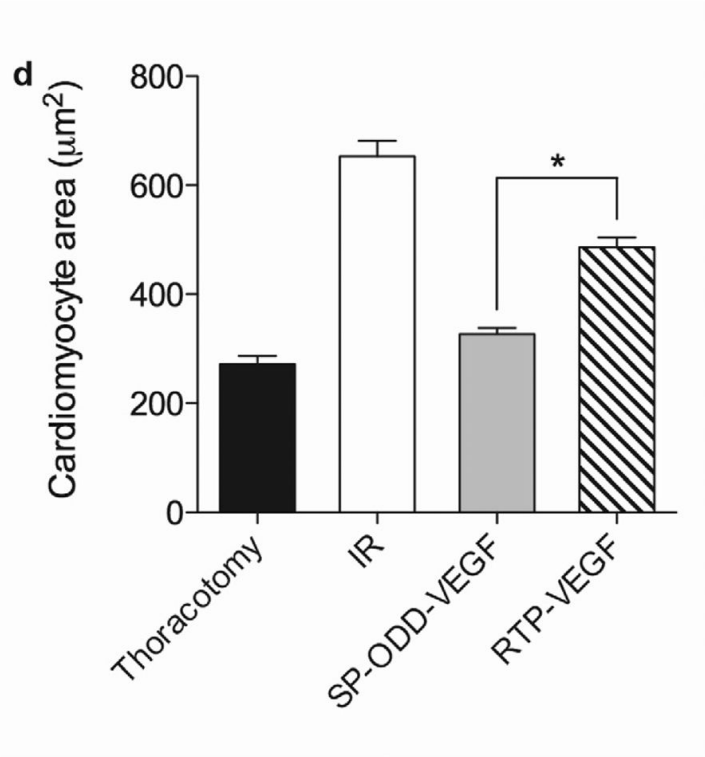

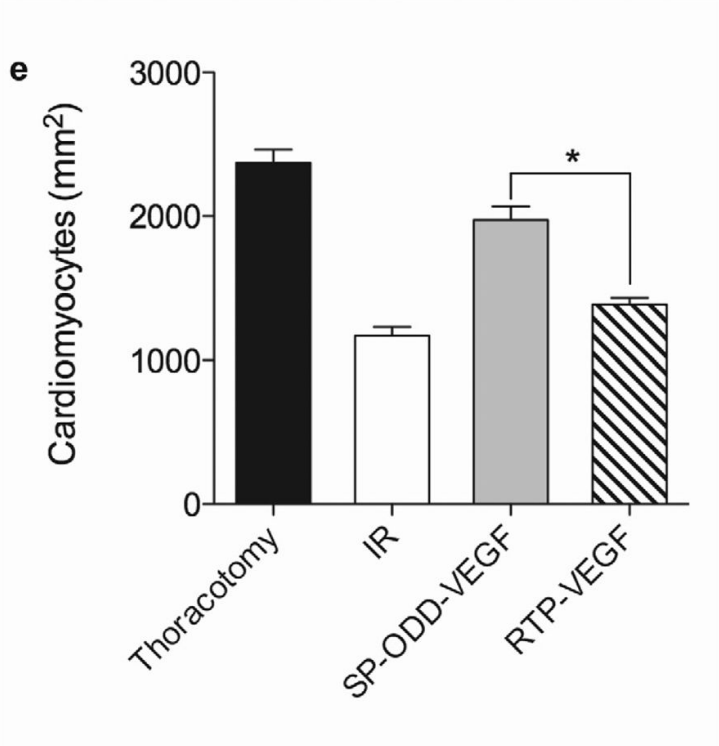

Figure 2.

Myocardial infarction, cardiomyocyte hypertrophy, and density. (a) Masson's trichrome (MT), TUNEL, and H&E staining. MT staining to visualize the area of infarction, TUNEL staining to determine apoptotic cardiomyocyte death, and H&E staining for general histological analysis were performed two weeks after surgery. (b) Analysis of the area of infarction. The infarct size was calculated as the percentage of infarcted tissue of the total area of the left ventricle. The data are presented as the mean ± the standard deviation (SD) of five animals per group (*p<0.05). (c) The number of TUNEL-positive cells. The TUNEL positive cells were counted in five random regions per sample in the ischemic border zone. (d) Cardiomyocyte hypertrophy. (e) Cardiomyocyte density. (*p<0.05, **p<0.01).

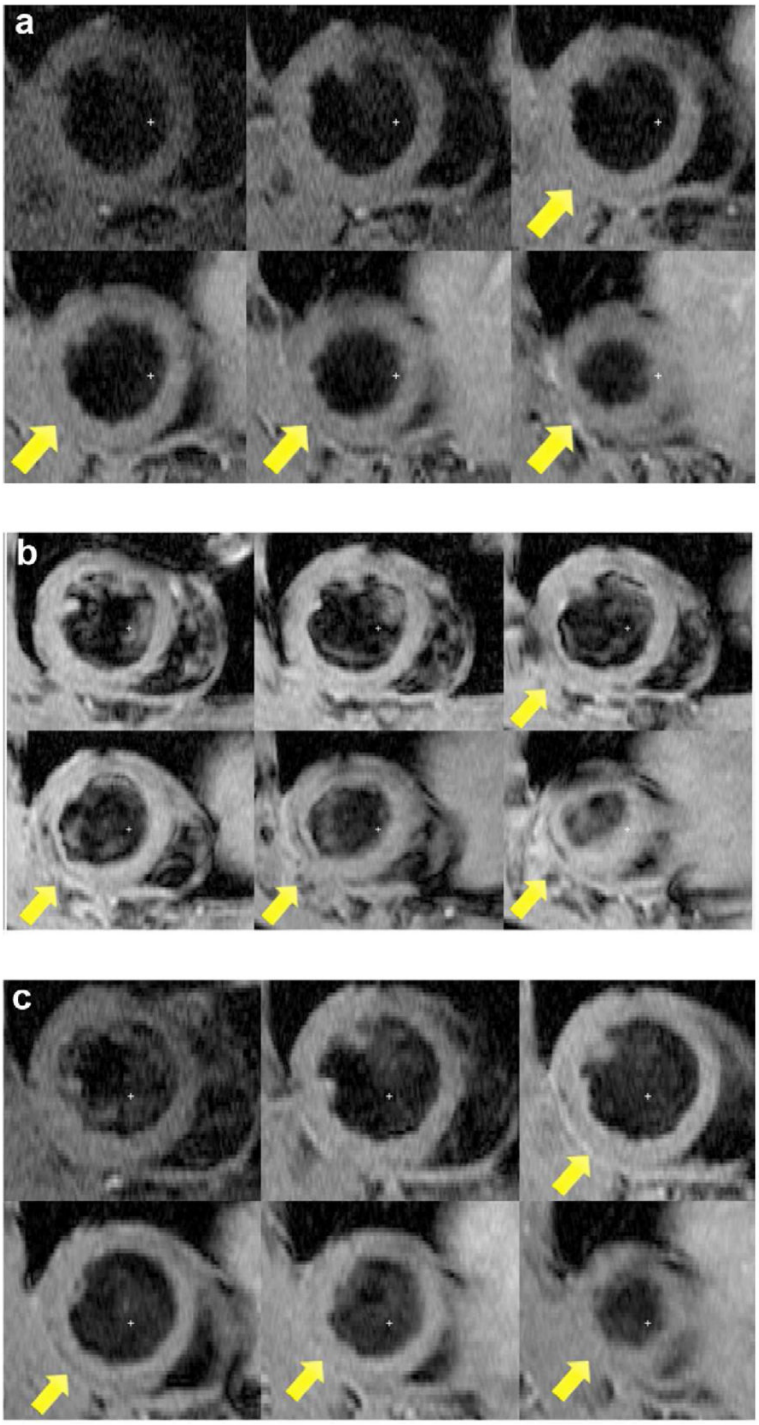

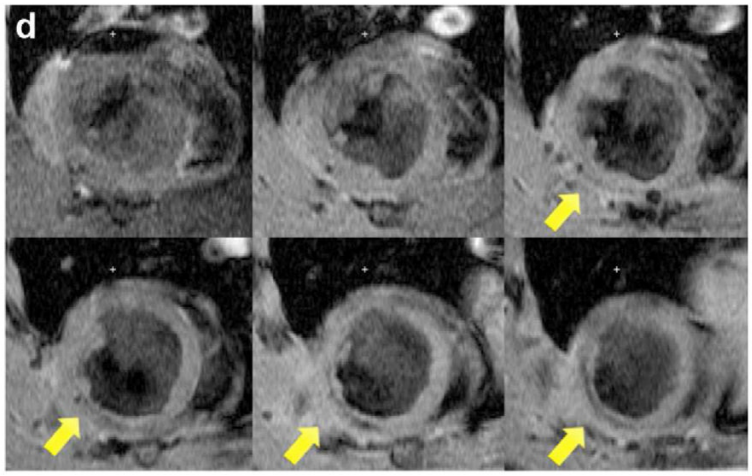

Figure 3.

Short axis MRI images of the left ventricles of the experimental groups. (a) Thoracotomy only, (b) Ischemia/Reperfusion (I/R), (c) pβ-SP-ODD-VEGF treatment, and (d) RTP-VEGF treatment groups. MRI analysis was performed to determine cardiac structure and function two weeks after surgery. Arrows indicate the regions of infarction in the left ventricles.

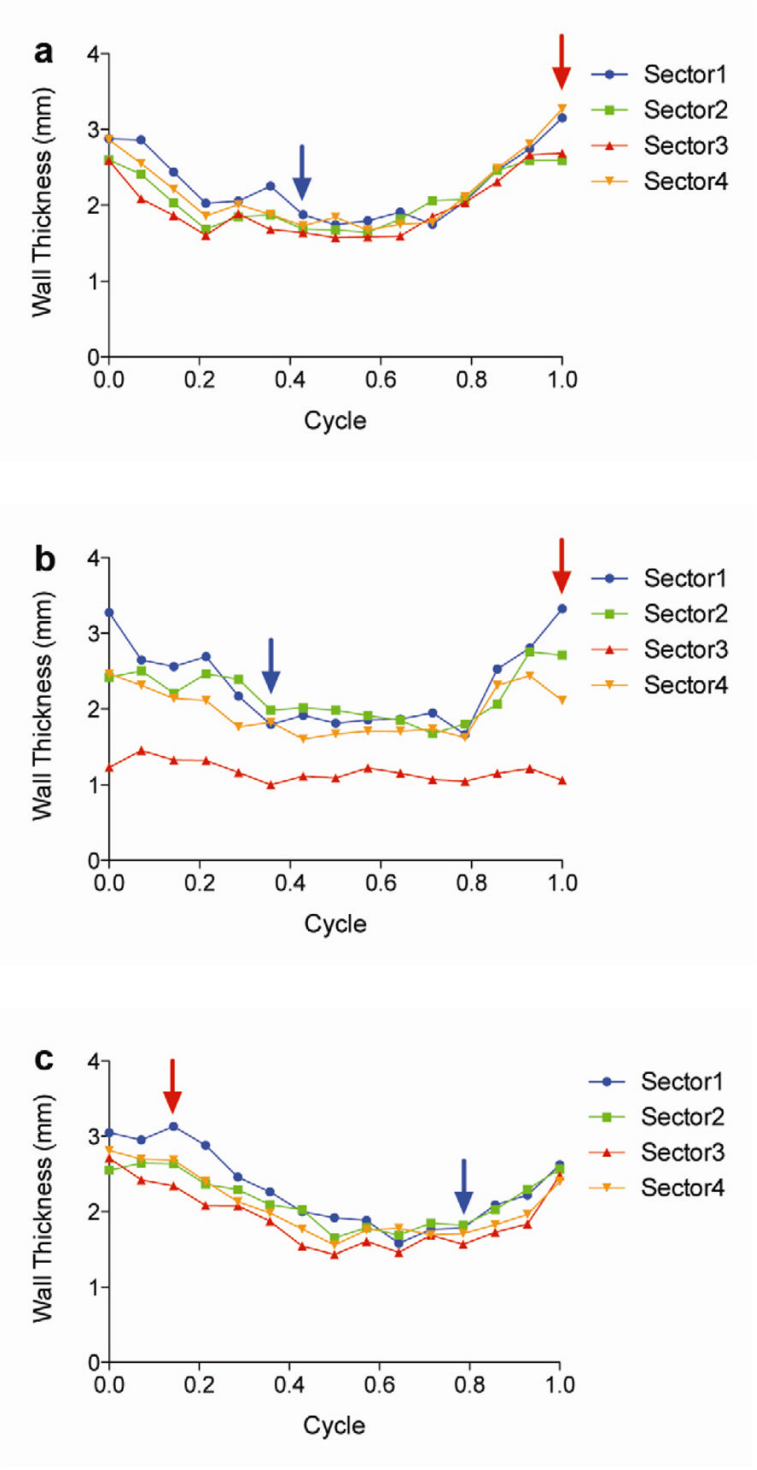

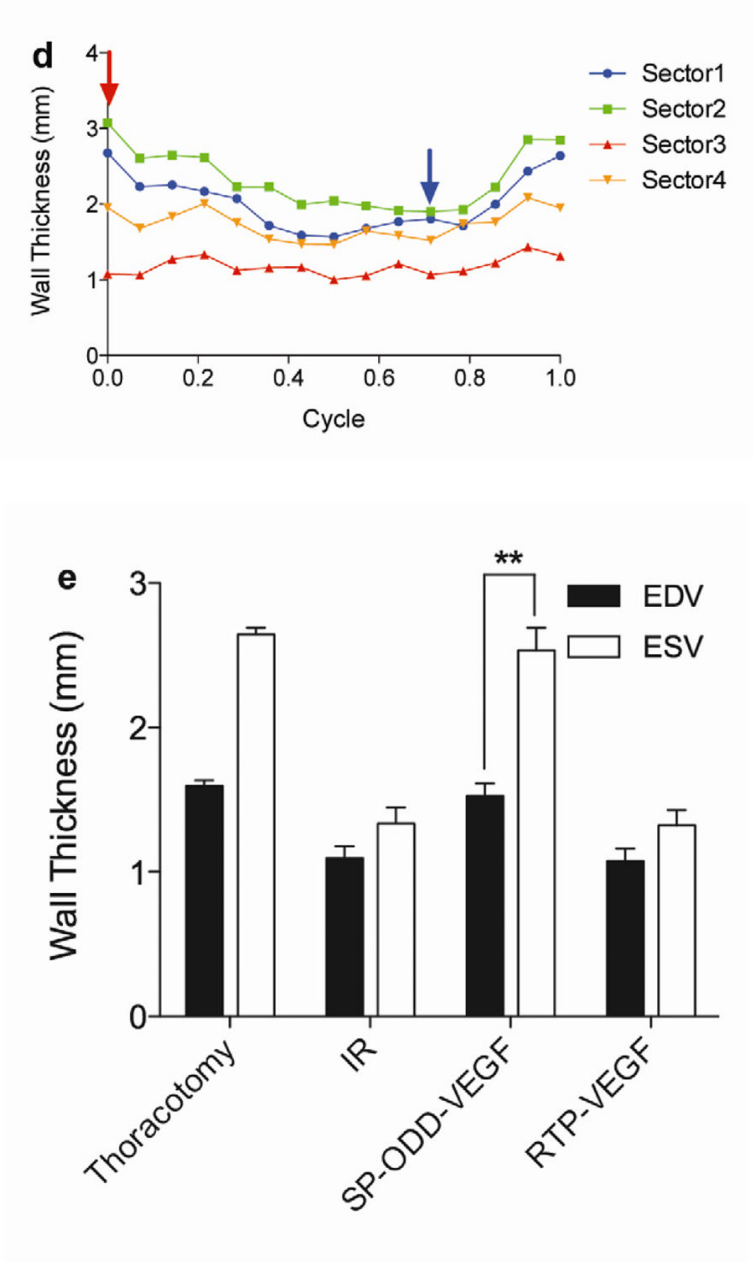

Figure 4.

Analysis of left ventricular wall thickness. Changes in wall thickness over time were determined by MRI analysis of (a) thoracotomy only, (b) Ischemia/Reperfusion (I/R), (c) pβ-SP-ODD-VEGF treatment, and (d) RTP-VEGF treatment groups. The left ventricles were divided into four sectors. Sector 3 indicates the wall thickness of the infarct area. The red arrows and the blue arrows indicate end diastolic and end systolic wall thickness, respectively. (e) Wall thickness of infarct area at end diastole and systole was measured by MRI analysis two weeks after surgery. Data presented as the mean + SD (**p<0.01).

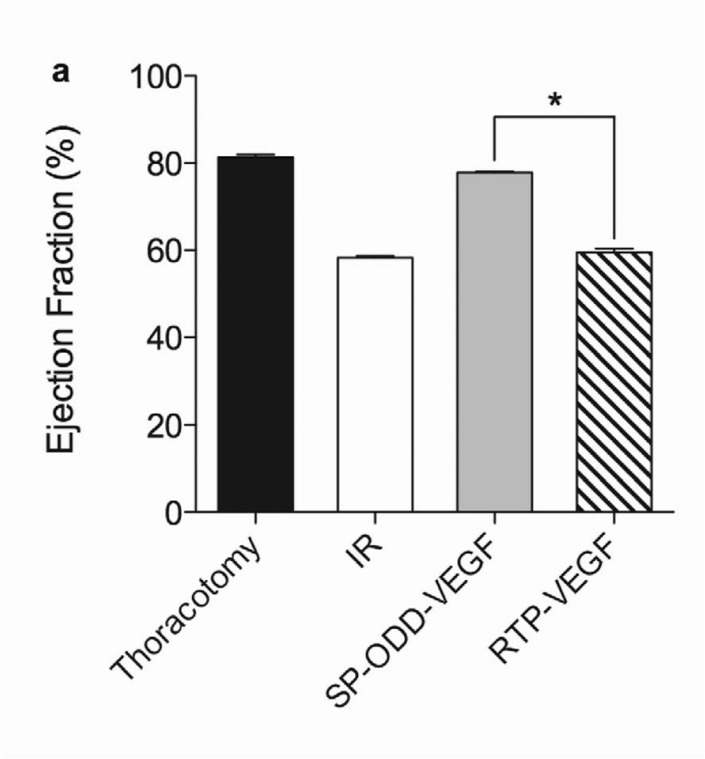

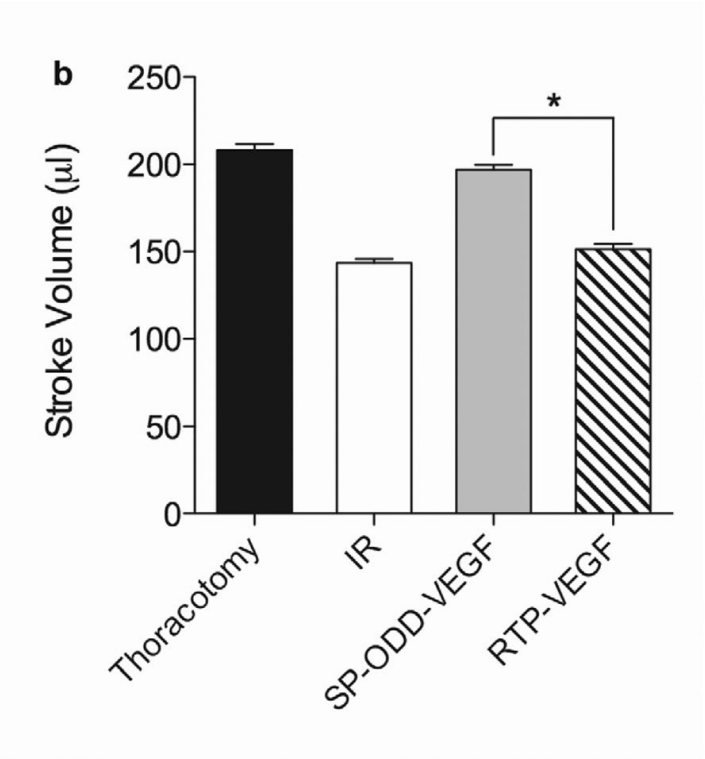

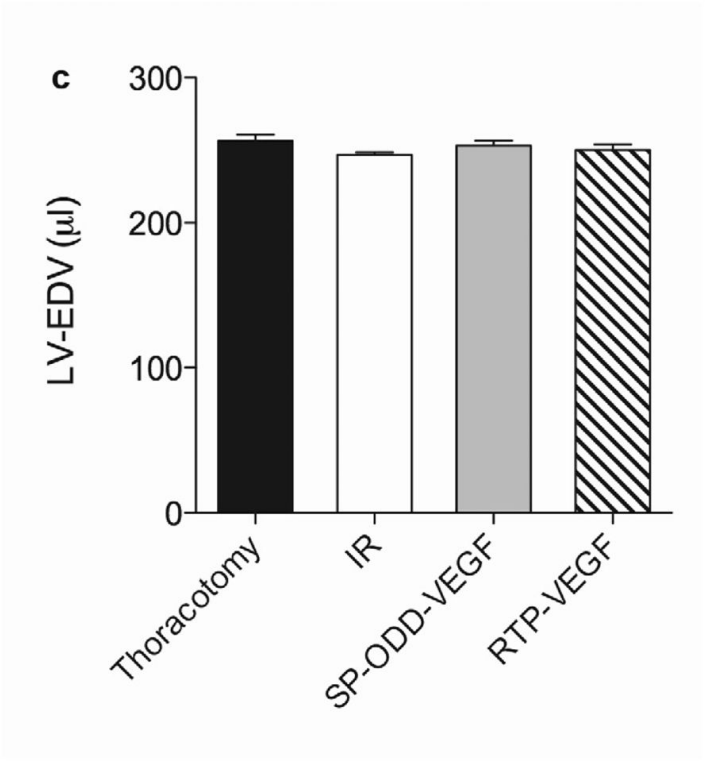

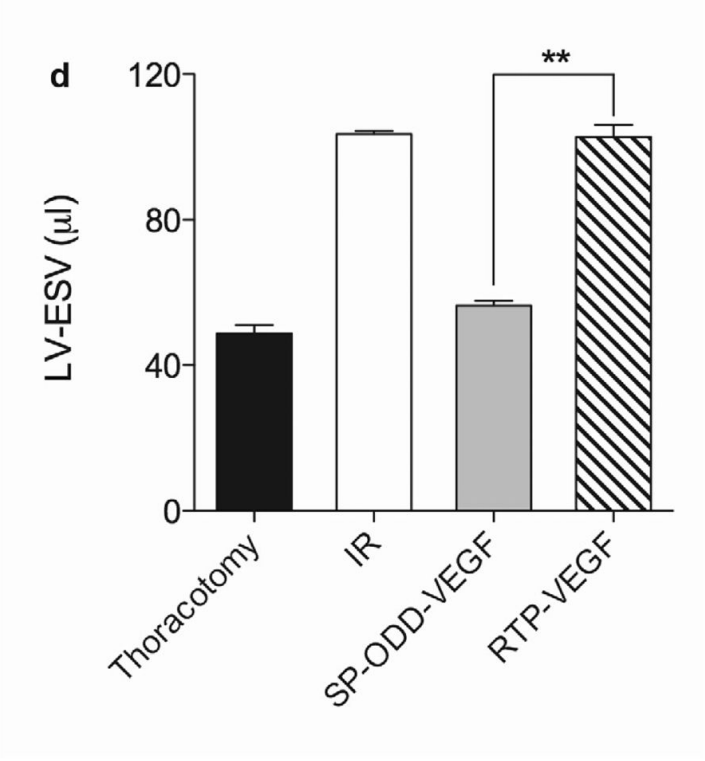

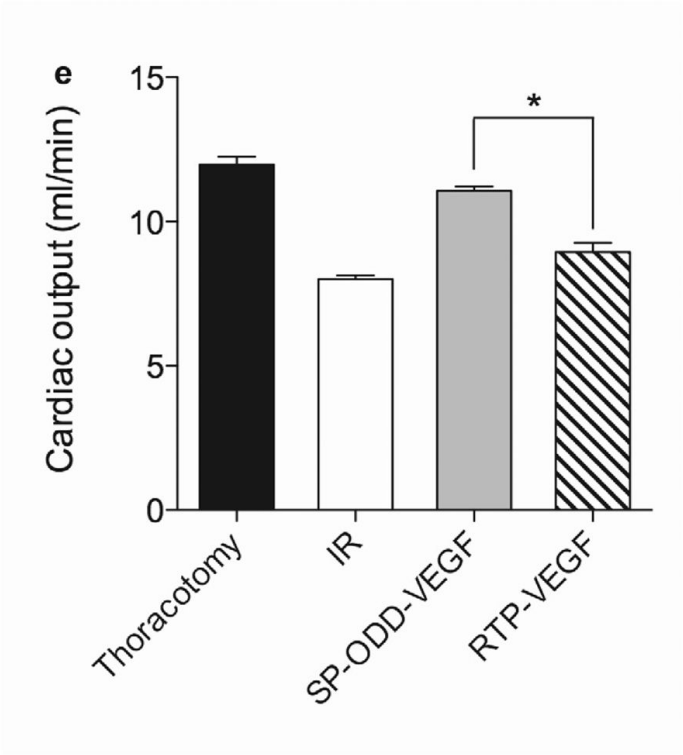

Figure 5.
Cardiac functional parameters determined by MRI analysis two weeks after surgery. (a) Cardiac ejection fraction, (b) stroke volume, (c) end diastolic volume (EDV), (d) end systolic volume (ESV), and (e) cardiac output. Data presented as the mean + SD (*$p<0.05$, **$p<0.01$).

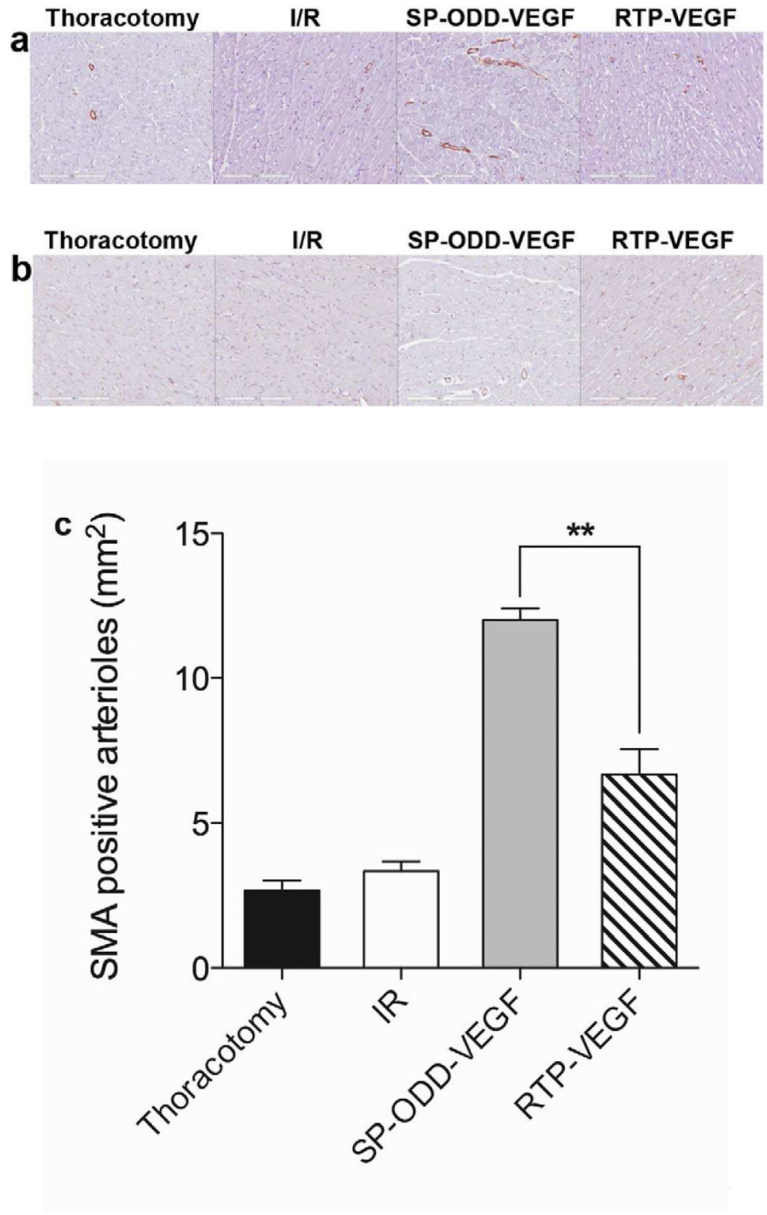

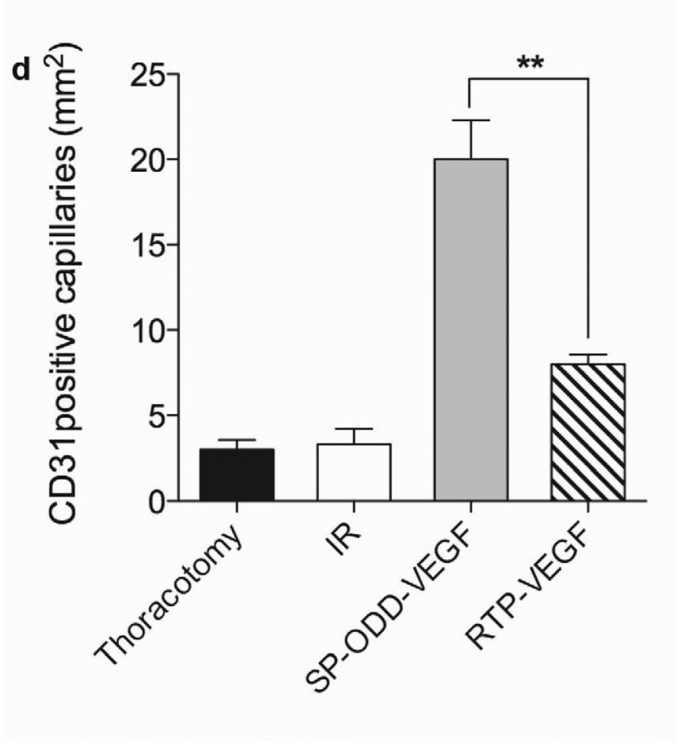

Figure 6.

Representative immunohistochemistry stain for micro vessel formation in the infarct border zone. Hearts were harvested immediately after the MRI analysis, and the isolated hearts were perfused, fixed, and sectioned through short axis. Immunohistochemical staining for (a) SM α-actin showing presence of arterioles and (b) CD31 detecting capillaries. (c) Average number of SMA positive arterioles and (d) average number of CD31 positive capillaries. The number of vessels in a 1 mm^2 area was recorded from five random high power fields in the infarct border zone per animal. Data presented as the mean + SD (**p<0.01).

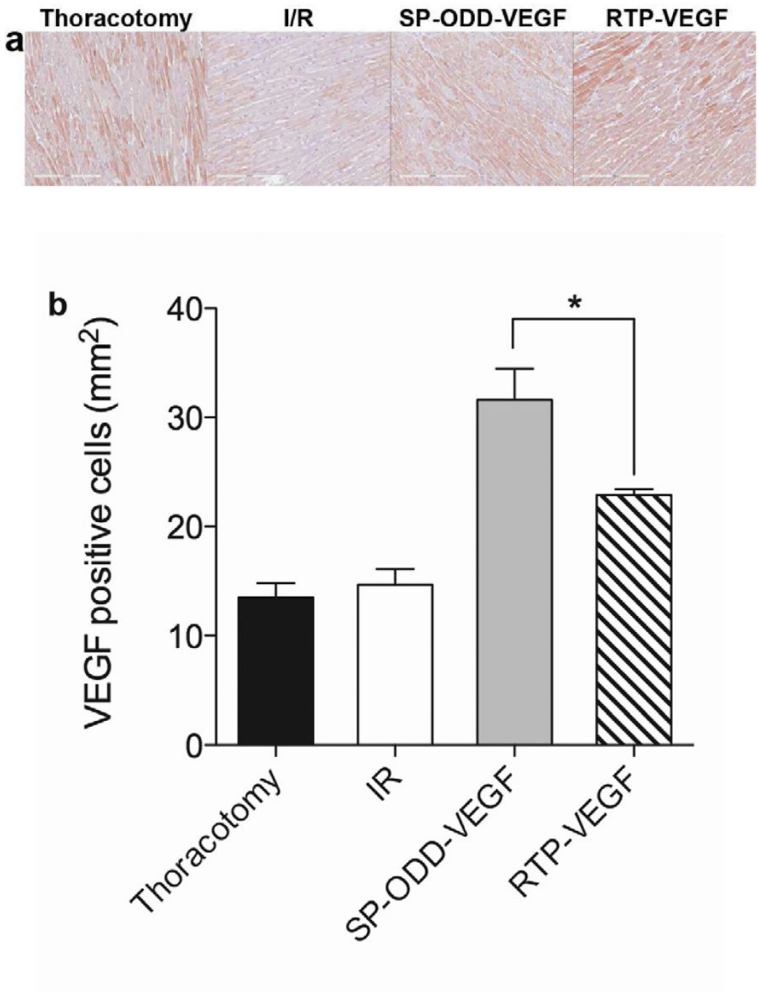

Figure 7.

VEGF expression in cardiomyocytes in the infarct border zone two weeks after surgery. (a) Immunohistochemical staining for VEGF showing VEGF positive cardiomyocytes stained dark pink. (b) Percentage of VEGF positive cells per mm^2 determined by Image J. Average values were obtained from five random high power fields in the infarct border zone per animal. Data presented as the mean + SD (*$p<0.05$).

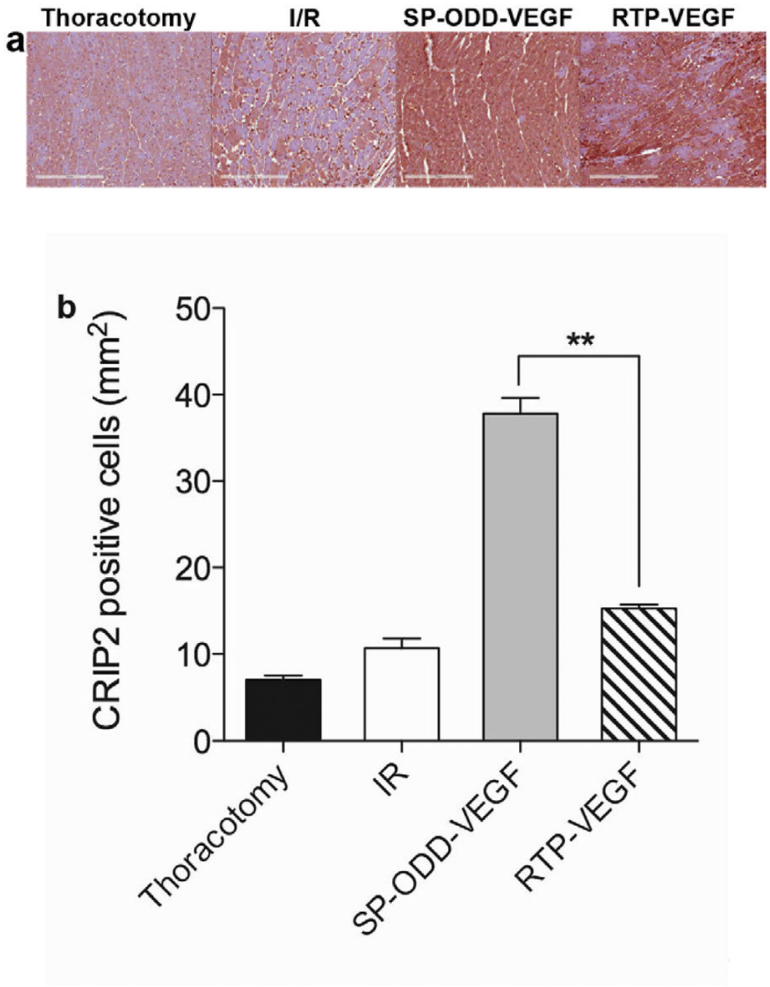

Figure 8.

CRIP2 expression showing smooth muscle cell development. (a) immunohistochemical staining for CRIP2 showing CRIP2 positive cardiomyocytes stained dark pink. (b) Percentage of CRIP2 positive cells per mm^2 determined by Image J. Average values were obtained from five random high power fields in the infarct border zone per animal. Data presented as the mean + SD (*p<0.05).